Available online at www.sciencedirect.com
SCIENCE DIRECT
Polymer 46 (2005) 9585–9595
polymer
www.elsevier.com/locate/polymer

Thiophene-containing poly(arylene–ethynylene)-*alt*-poly(arylene–vinylene)s: Synthesis, characterisation and optical properties

Daniel Ayuk Mbi Egbe[a,*], Le Huong Nguyen[b], Benjamin Carbonnier[c], David Mühlbacher[d], Niyazi Serdar Sariciftci[b]

[a]*Institut für Organische Chemie und Makromolekulare Chemie der Friedrich-Schiller Universität Jena, Humboldtstr. 10, D-07743 Jena, Germany*
[b]*Linz Insitute for Organic Solar Cells (LIOS), Johannes Kepler University, Altenbergerstr. 69, A-4040 Linz, Austria*
[c]*Laboratoire de Recherche sur les Polymères, CNRS-UMR 7581, 2-8 rue Henri Dunant, 94320 Thiais, France*
[d]*Konarka Austria, Forschungs-und Entwicklungs GmbH, Gruberstr. 40-42, A-4020 Linz, Austria*

Received 26 May 2005; received in revised form 31 July 2005; accepted 2 August 2005
Available online 19 August 2005

Abstract

This work describes the synthesis and characterisation of two types of thiophene-containing poly(arylene–ethynylene)-*alt*-poly(arylene–vinylene)s (PAE–PAV) copolymers, whose repeating units (–Ph–C≡C–Th–CH=CH–Ph–CH=CH–)$_n$, **5**, and (–Th–C≡C–Ph–C≡C–Th–CH=CH–Ph–CH=CH–)$_n$, **8a–c**, consist, respectively, of a 1:2 and a 2:2 ratio of triple bond/double bond moieties. Comparison of their photophysical, electrochemical and photovoltaic properties has been carried out. Although similar electrochemical data (HOMO: −5.43 eV, LUMO: ∼ −3.15 eV, $E_g^{ec} = 2.28$ eV) as well as identical thin film absorption behaviour ($\lambda_a = 500$ nm, $E_g^{opt} = 2.10$ eV) were obtained for both types of materials, significant differences in their thin film photoluminescence behaviour and photovoltaic properties were observed. While polymer **5** shows a fluorescence maximum at $\lambda_e = 568$ nm (with a fluorescence quantum yield of $\Phi_f = 7\%$), a total fluorescence quenching was observed in **8**. Far better photovoltaic performance was obtained from solar cells (set up: ITO/PEDOT:PSS/active layer/LiF/Al; active layer consisting of **5** or **8b** as donor and PCBM as acceptor in a 1:3 ratio by weight) designed from **5** than from **8b**. Open circuit voltage, V_{OC}, as high as 900 mV and power conversion efficiency, $\eta_{AM1.5}$, around 1.2% were obtained. This can be attributed to the 1:2 triple bond/double bond ratio as well as the grafting of shorter octyloxy and 2-ethylhexyloxy side chains in **5** and to its comparatively higher molecular-weight.

Keywords: Photoactive polymers; Organic photovoltaic devices; Thiophene-containing PPV derivatives

1. Introduction

Organic photovoltaic devices can be seen as part of the worldwide effort towards renewable energy sources [1–4]. Their easy processability into flexible, lightweight and efficient solar cell devices make them a potential alternative to conventional inorganic photovoltaic devices. The first report of ultrafast photoinduced femtosecond charge transfer from a poly(*p*-phenylene–vinylene) derivative to the Buckminsterfullerene by Sariciftci et al. in 1992 resulted in worldwide efforts to use this phenomenon in organic photovoltaic devices [5]. Upon photoexcitation of an electron–hole pair, the transfer of electrons from the polymer (donor) onto the fullerene (acceptor) leads to an efficient separation of charges [6] (facilitated by a slow microsecond recombination) [1] that is required in photovoltaic devices.

Polythiophenes, e.g. poly(3-hexylthiophene), have been proven to be efficient donor materials for photovoltaic devices delivering high short circuit currents, I_{SC}, of up to 10 mA/cm^2, attributed to high degree of intermolecular ordering leading to high charge carrier mobility [7–9]. Power conversion efficiencies of up to 3.5% have been reported [8]. The open circuit voltage, V_{OC}, of such devices generally does not exceed 650 mV [8,10]. Whereas poly(arylene–ethynylene)-*alt*-poly(arylene–vinylene) (PAE–PAV) based solar cell devices have shown higher V_{OC}'s [11–15]. The combination of both types of structures within unique conjugated polymeric backbone may offer a path to new class of polymers for high performance photovoltaic

* Corresponding author. Tel.: +49 3641 948247; fax: +49 3641 948202.
E-mail address: c5ayda@uni-jena.de (D.A.M. Egbe).

0032-3861/$ - see front matter © 2005 Elsevier Ltd. All rights reserved.
doi:10.1016/j.polymer.2005.08.008

devices. In this line, we report on the synthesis of a thiophene-containing PAE–PAV **5** (Scheme 1). The choice and positioning of the side chains are presumed not only to enable high solubility of the material in usual organic solvents but also to facilitate the charge transfer from **5** to the acceptor PCBM. Moreover the 1:2 triple bond/double bond ratio should guarantee a better intramolecular charge carrier mobility compared to polymers **8** [16] with a 2:2 ratio (Scheme 2) [11,15]. A comparison of the solution and solid state photophysical properties as well as the electrochemical properties of **5** and **8b** has been carried out. Results from photovoltaic investigations based on polymer **5** and **8b** are presented.

2. Experimental

2.1. Instrumentation

^{1}H NMR and ^{13}C NMR were measured in deuterated chloroform on a Bruker DRX 400 and a Bruker AC 250 using tetramethylsilane as internal standard. The elemental analysis was performed on a CHNS-932 Automat Leco. Infrared spectroscopy was recorded on a Nicolet Impact 400. Differential scanning calorimetry (DSC) experiments were conducted with cooling and heating rates of 10 °C/min using a Mettler 30 calorimeter with a cell purged with nitrogen. The second heating run is considered as reflecting the properties of the compact bulk material. Wide-angle X-ray diffraction (WAXS) patterns were recorded using the X-ray beam with a pinhole collimation and a two-dimensional detector (Siemens Serial A102647) with 1024×1024 pixel. A double graphite monochromator for the Cu Kα radiation (λ= 0.154 nm) was used. The beam diameter was about 0.5 mm and the sample to detector distance was 80 mm. The recorded scattered intensity distributions were integrated over the azimuthal angle and are presented as function of the scattering vector ($s=2\sin\theta/\lambda$, where 2θ is the scattering angle). Gel permeation chromatography (GPC) was performed on a set of Knauer using THF as eluent and polystyrene as standard. The absorption spectra were recorded in dilute chloroform solution (10^{-5}–10^{-6} M) on a Perkin–Elmer UV/vis-NIR Spectrometer Lambda 19. Quantum-corrected emission spectra were measured in dilute chloroform solution (10^{-6} M) with a LS 50 luminescence spectrometer (Perkin–Elmer). The fluorescence quantum yields (error $<\pm 10\%$) were calculated relative to quinine sulfate (purum, Fluka) in 0.1 N H_2SO_4 (pro analysi; Laborchemie Apolda) used a standard (Φ_f=55%). The absorbance at the excitation wavelength was kept below 0.05 for the samples and the reference. The solid-state absorption and emission were measured using Hitachi F-4500 Fluorescence Spectrophotometer. The films were spin-casted from a chlorobenzene solution (10^{-2}–10^{-3} M). Fluorescence quantum yields in solid state were determined against a CF_3P-PPV copolymer reference whose quantum yield has been measured by an intergrating sphere to be 43% [17].

The experimental details of electrochemical studies are similar to those reported elsewhere [12].

2.2. Experimental conditions for solar cells

Blend solutions of either polymer **5** or **8b** as donor component and the C_{60}-derivative 1-(3-methoxycarbonyl) propyl-1-phenyl [6,6] C_{61} (PCBM) as acceptor at a weight ratio of 1:3 were prepared in chloroform at a concentration of 10 mg polymer/mL. Poly(3,4-ethylenedioxythiophene): poly(styrenesulfonate) (PEDOT:PSS) (Baytron PH, Bayer Germany) was spin-coated on top of indium-tin oxide (ITO) (Merck, Germany) coated glass ($\sim$25 V/cm^2), which had been cleaned in an ultrasonic bath with acetone and isopropyl alcohol after etching part of the ITO glass. Then the active layer (polymer: PCBM blend) was spin-coated on the annealed PEDOT: PSS layer (about 80 nm thick). Six angstrom of lithium fluoride (LiF) and 80 nm thick Al electrode was deposited on the blend film by thermal evaporation at $\sim 5\times10^{-6}$ mbar. All current–voltage (*I–V*) characteristics of the photovoltaic devices were measured using a Keithley SMU 2400 unit under inert atmosphere (argon) in a dry glove box. A Steuernagel solar simulator under AM 1.5 conditions was used as the excitation source with an input power of 100 mW/cm^2 white light illumination.

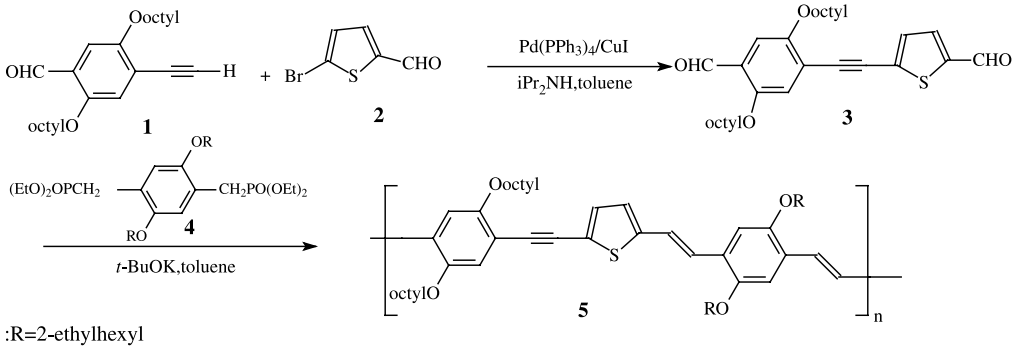

Scheme 1.

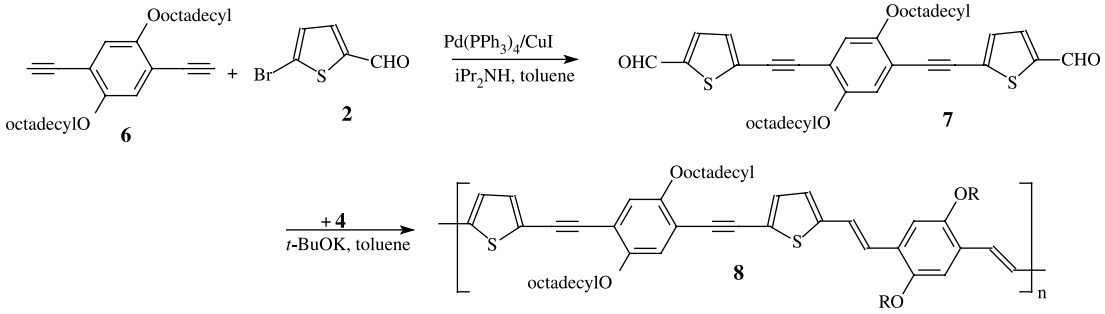

8a:R=octadecyl, **8b**:R=dodecyl, **8c**:R=octyl

Scheme 2.

2.3. Materials

All starting materials were purchased from commercial suppliers (Fluka, Merck and Aldrich). Toluene, tetrahydrofurane and diethyl ether were dried and distilled over sodium and benzophenone. Diisopropylamine was dried over KOH. If not otherwise specified the solvents were degassed by bubbling with argon or nitrogen 1 h prior to use.

4-Formyl-2,5-dioctylphenylacetylene (**1**) [17c] 2,5-dialkoxy-*p*-xylylene-bis(diethylphosphonate) (**4**) [17a,b] and 1,4-diethynyl-2,5-dioctadecyloxybenzene (**6**) [18] have been described elsewhere.

2.3.1. 1-(4-Formyl-2,5-dioctyloxyphenyl)-2-(5-formylthiophene-2-yl)-acetylene (*3*)

4-Formyl-2,5-dioctyloxyphenylacetylene (**1**) [17c] (1.45 g, 3.871 mmol), 5-bromothiophene-2-carboxaldehyde (**2**) (741 mg, 3.871 mmol), $Pd(PPh_3)_4$ (179 mg, 0.15 mmol) and CuI (29.5 mg, 0.15 mmol) were given to a degassed solution of diisopropylamine (20 ml) and toluene (40 ml). The reaction mixture was heated at 70–80 °C for 24 h. After filtration of the precipitated ammonium bromide salt, the solvent was removed under vacuum. The residue was chromatographed on a 300 g silica gel 60 column using toluene as eluent. The expected product **3** was detected on TLC at $R_f = 0.58$ and was obtained as a pale yellow crystalline substance. Yield: 1.3 g (68%). Mp: 95–110 °C. ^{1}H NMR (250 MHz, $CDCl_3$): δ (ppm) = 0.77 → 1.82 (30H, m, $CH_3(CH_2)_6$–), 3.94 → 4.01 (4H, m, –CH_2O–), 7.03 and 7.19 (2H, phenylene H's), 7.32 and 7.62 (2H, thiophene H's), 9.82 and 10.38 (2H, –CHO). ^{13}C NMR (62 MHz, $CDCl_3$): δ (ppm) = 14.12 (CH_3), 22.67 → 31.80 (–$(CH_2)_6$–), 69.31, 69.35 (–CH_2O–), 89.11 and 93.93 (–C≡C–), 109.96 → 155.33 (arylene C's), 182.40 and 189.11 (–CHO). FT-IR: 2920 and 2853 (vs, CH_3–, –CH_2–), 2199.95 (m, –C≡C–), 1670 (vs, –CHO), 1603 (s, arylene –C=C–), 1210 (vs, Ar-OR). λ_{max} (nm) (ε (L/mol cm)) 276.0 (10,950), 348.8 (25,750), 401.6 (22,000). Anal. Calcd for $C_{30}H_{40}SO_4$ (496.71): C, 72.54; H, 8.12; S, 6.46. Found: C, 72.23; H, 8.12; S, 6.16.

2.3.2. Poly{1,4-(2,5-dioctyl)phenylene-ethynylene-thiophene-2,5-ylene-vinylene-1,4-[2,5-bis-(2′-ethyl)hexyloxy] phenylene-vinylene} (*5*)

Dialdehyde **3** (1 g, 2.01 mmol) and 2,5-bis(2′-ethylhexyloxy)-*p*-xylylene-bis(diethylphosphonate) [17b] (**4**) (1.28 mg, 2.01 mmol) were dissolved in toluene (20 mL) while stirring vigorously under argon and heating under reflux. Potassium *tert*-butoxide (670 mg, 6.0 mmol) was added to this solution; and the reaction mixture was heated at reflux for 3 h. Within this time, additional toluene (10 mL) was added in small portions due to the fast increase of viscosity of the reaction mixture. After this time, more toluene was added and the reaction was quenched with aqueous HCl. The organic phase was separated and extracted several times with distilled water until the water phase became neutral (pH = 6–7). The organic layer was dried in a Dean–Stark apparatus. The resulting toluene suspension was filtered and evaporated under vacuum to the minimum (80 mL) and precipitated in methanol (400 mL). The polymer was dissolved in 30 mL toluene and reprecipitated in 300 mL acetone. After extraction with hot methanol and drying under vacuum, 600 mg of dark red material were obtained. Yield: 37%. GPC (THF): $M_w = 74{,}000$ g/mol, $M_n = 28{,}000$ g/mol, $M_z = 184{,}000$ g/mol polydispersity index (PDI) = 2.68. ^{1}H NMR (250 MHz, $CDCl_3$): δ (ppm) = 0.80 → 1.78 (60H, m, alkyl side chains-), 3.88 → 4.01 (8H, br, –CH_2O–), 6.93 → 7.42 (10H, arylene and vinylene H's). ^{13}C NMR (62.9 MHz, $CDCl_3$): δ (ppm) = 11.33 and 14.07 (CH_3), 22.65 → 31.83 (–(CH_2)– units), 39.74 (–CH– unit), 69.43, 69.66, 71.66 (–CH_2O–), 88.02, 91.53 (–C≡C–), 110.19 → 154.08 (arylene and vinylene C's). FT-IR: 3062 and 3039 (vw, aromatic C–H), 2959, 2923 and 2855 (vs, CH_3 and –CH_2–), 2189 (vw, disubst. –C≡C–), 1673 (vw, CHO), 1599 (vw,-arylene –C=C–),1200 (s, C_{phenyl}–OR), 967 (s, trans–CH=CH–) cm^{-1}. UV–vis ($CHCl_3$): λ_{max} (nm) (ε (L/mol cm)) 487 (37,800). Anal. Calcd for $(C_{54}H_{78}O_4S)_n$ $(823.27)_n$:C, 78.78; H, 9.55; S, 3.89. Found: C, 75.25; H, 9.62; S, 3.44.

*2.3.3. 1,4-Dioctadecyloxy-2,5-bis(5-formylthiophene-2-yl ethynyl)benzene (**7**)*

1,4-Diethynyl-2,5-dioctadecyloxybenzene (**6**) [18] (3.78 g, 5.7 mmol), $Pd(PPh_3)_4$ (280 mg, 0.24 mmol) and CuI (46 mg, 0.24 mmol) were given to a degassed solution of 5-bromothiophene-2-carboxaldehyde (**2**) (2.8 g, 14.7 mmol) in diisopropylamine (60 ml) and toluene (80 ml). The reaction mixture was heated at 70–80 °C for 24 h. After filtration of the precipitated ammonium bromide salt, the solvent was removed under vacuum. The residue was chromatographed on silica gel 60 column using toluene as eluent. The expected product **7** was detected on TLC at R_f = 0.45 and was obtained as yellow crystalline substance. Yield: 3.3 g (68%). Mp: 89–90 °C. ^{1}H NMR (250 MHz, $CDCl_3$): δ (ppm) = 0.80 (6H, t, ^3J = 6.50 Hz, CH_3–), 1.17 → 1.80 (64H, m, –(CH_2)$_{16}$–), 3.95 (4H, t, ^3J = 6.36 Hz, –CH_2O–), 6.93 (2H, s, phenylene H's), 7.23 (2H, d, ^3J = 3.92 Hz, thiophene H), 7.60 (2H, d, ^3J = 3.92 Hz, thiophene H), 9.80 (2H, –C*H*O). ^{13}C NMR (62.9 MHz, $CDCl_3$): δ (ppm) = 14.13 (*C*H$_3$), 22.70 → 31.93 (–(*C*H$_2$)$_{16}$–), 69.63 (–*C*H$_2$O–), 87.78 and 94.54 (–C≡C–), 113.67 → 153.81 (arylene C's), 182.31 (–*C*HO). UV–vis ($CHCl_3$): λ_{max} (nm) (ε (L/mol cm)) 271.2 (17,700), 347.2 (31,500), 415.2 (44,400). Anal. Calcd for $C_{56}H_{82}S_2O_4$ (496.71): C, 76.14; H, 9.36; S, 7.26. Found: C, 76.17; H, 10.32; S, 6.73.

*2.3.4. Poly[2,5-thiopheneethynylene-1,4-(2,5-dioctadecyloxyphenylene)ethynylene-2,5-thiophene-vinylene-1,4-(2,5-dioctyloxyphenylene)vinylene] (**8c**)*

Dialdehyde **7** (598 mg, 0.68 mmol) and 2,5-dioctyloxy-*p*-xylylene-bis(diethylphosphonate) [17b] (**4c**) (433 mg, 0.68 mmol) were dissolved in 20 ml dried toluene while stirring vigorously under argon and heating under reflux. After adding potassium *tert*-butoxide (230 mg; 2.05 mmol) to this solution, the reaction mixture was heated at reflux for 2 h. After this time the reaction was quenched with 25 ml aqueous HCl (5%). The organic phase was separated and extracted several times with distilled water until the water phase became neutral. The organic layer was dried in a Dean–Stark-apparatus. The resulting toluene solution was evaporated under vacuum to about 50 ml and precipitated in dry methanol. The polymer was extracted 8 h with methanol and dried under vacuum. 610 mg (73%) of red polymer were obtained. GPC (THF): M_w = 13,000 g/mol, M_n = 4400 g/mol, M_z = 30,000 g/mol, PDI = 2.95. ^{1}H NMR (250 MHz, $CDCl_3$): δ (ppm) = 0.77 → 1.78 (94H, m, alkyl side chains-), 3.14 (d, ^3J = 22.5 Hz end group phosphonate), 3.88 → 4.02 (8H, –CH_2O–), 6.74 → 7.23 (12H, arylene and vinylene H's). ^{13}C NMR (62.9 MHz, $CDCl_3$): δ (ppm) = 14.14, 16.35 (*C*H$_3$), 22.71 → 31.94 (–(*C*H$_2$)–units), 61.90, 69.46, 69.69 (–*C*H$_2$O–), 88.93, 91.08 (–C≡C–), 110.57 → 153.52 (arylene and vinylene C's). UV–vis ($CHCl_3$): λ_{max} (nm) (ε (L/mol cm)) 326 (13,400), 476.2 (58,600). Anal. Calcd for $(C_{80}H_{124}O_4S_2)_n$ (1214.00)$_n$:C, 79.15; H, 10.30; S, 5.28. Found: C, 77.24; H, 10.97; S, 4.88.

*2.3.5. Poly[2,5-thiopheneethynylene-1,4-(2,5-dioctadecyloxyphenylene)ethynylene-2,5-thiophene-vinylene-1,4-(2,5-dioctadecyloxyphenylene)vinylene] (**8a**)*

Dialdehyde **7** (601 mg, 0.68 mmol) and 2,5-dioctyloxy-*p*-xylylene-bis(diethylphosphonate) [17a,b] (**4a**) (624 mg, 0.68 mmol) were dissolved in 20 ml dried toluene while stirring vigorously under argon and heating under reflux. Potassium *tert*-butoxide (229 mg; 2.04 mmol) was added to this solution. The reaction mixture was heated at reflux for 2 h. After this time the reaction was quenched with 25 ml aqueous HCl (5%). The work up was done as described above. Thus, 800 mg (79%) of a red polymer was obtained. GPC (THF): M_w = 19,700 g/mol, M_n = 8000 g/mol, M_z = 40,600 g/mol, PDI = 2.46. ^{1}H NMR (250 MHz, $CDCl_3$): δ (ppm) = 0.77 → 1.78 (140H, m, alkyl side chains-), 3.14 (d, ^3J = 22.5 Hz end group phosphonate), 3.91 → 3.97 (8H, –CH_2O–), 6.88 → 7.23 (12H, arylene and vinylene H's). UV–vis ($CHCl_3$): λ_{max} (nm) (ε (L/mol cm)) 251.6 (15,200), 477 (59,000). Anal. Calcd for $(C_{100}H_{164}O_4S_2)_n$ (1494.54)$_n$:C, 80.37; H, 11.06; S, 4.29. Found: C, 78.78; H, 12.16; S, 3.80.

*2.3.6. Poly[2,5-thiopheneethynylene-1,4-(2,5-dioctadecyloxyphenylene)ethynylene-2,5-thiophene-vinylene-1,4-(2,5-didodecyloxyphenylene)vinylene] (**8b**)*

Dialdehyde **7** (600 mg, 0.68 mmol) and 2,5-didodecyloxy-*p*-xylylene-bis(diethylphosphonate) [17a,b] (**4b**) (508 mg, 0.68 mmol) were dissolved in 20 ml dried toluene while stirring vigorously under argon and heating under reflux. Potassium *tert*-butoxide (229 mg; 2.04 mmol) was added to this solution. The reaction mixture was heated at reflux for 2 h. After this time the reaction was quenched with 25 ml aqueous HCl (5%). The workup was done as described above. Thus, 700 mg (78%) of a red polymer were obtained. GPC (THF): M_w = 20,000 g/mol, M_n = 9000 g/mol, M_z = 40,000 g/mol PDI = 2.22. ^{1}H NMR (250 MHz, $CDCl_3$): δ (ppm) = 0.77 → 1.78 (140H, m, alkyl side chains-), 3.14 (d, ^3J = 22.5 Hz end group phosphonate), 3.96 (8H, –CH_2O–), 6.88 → 7.23 (12H, arylene and vinylene H's). ^{13}C NMR (62.9 MHz, $CDCl_3$): δ (ppm) = 14.09 (*C*H$_3$), 22.67 → 31.91 (–(*C*H$_2$)– units), 69.45, 69.68 (–*C*H$_2$O–), 88.90, 91.06 (–C≡C–), 110.62 → 153.52 (arylene and vinylene C's). FT-IR: 2923 and 2849 (vs, CH_3 and –CH_2–), 2187 (vw, disubst. –C≡C–), 1673 (vw, CHO), 1599 (vw,-arylene –C=C–),1215 (s, C_{phenyl}–OR), 951 (s, trans–CH=CH–) cm^{-1}. UV–vis ($CHCl_3$): λ_{max} (nm) (ε (L/mol cm)) 254.6 (11,700), 476 (51,100). Anal. Calcd for $(C_{88}H_{140}O_4S_2)_n$ (1326.22)$_n$:C, 79.70; H, 10.64; S, 4.84. Found: C, 78.11; H, 12.03; S, 4.53.

*2.3.7. 2,5-Bis(4-formyl-2,5-dioctyloxyphenylethynyl)thiophene (**10**)*

4-Formyl-2,5-dioctyloxyphenylacetylene (**1**) [17c] (4.005 g, 10.37 mmol), 2,5-dibromothiophene (**9**) (633 mg, 4.91 mmol), $Pd(PPh_3)_4$ (218 mg, 0.189 mmol, 4 mol%) and CuI (36 mg, 0.189 mmol) were given to a degassed solution

of diisopropylamine (75 ml) and toluene (50 ml). The reaction mixture was heated at 70–80 °C for 24 h. After filtration of the precipitated ammonium bromide salt, the solvent was removed under vacuum. The residue was chromatographed on a silica gel 60 column using toluene as eluent. The expected product **10** was detected on TLC at $R_f = 0.75$ and was obtained as a pale yellow crystalline substance. Yield: 2.5 g (60%). Mp: 81–90 °C. ^{1}H NMR (250 MHz, $CDCl_3$): δ (ppm) = 0.84 → 1.85 (60H, m, $CH_3(CH_2)_6$–), 3.98 → 4.07 (8H, m, –CH_2O–), 7.03 and 7.18 (2H, phenylene H's), 7.3 (2H, d, $^3J = 2.40$ Hz thiophene H's), 10.42 (2H, –CHO). ^{13}C NMR (62 MHz, $CDCl_3$): δ (ppm) = 14.05 (CH_3), 22.62 → 31.76 (–$(CH_2)_6$–), 69.31, 69.54 (–CH_2O–), 89.72 and 90.79 (–C≡C–), 110.01 → 153.61, 155.48 (arylene C's), 189.03 (–CHO). Anal. Calcd for $C_{54}H_{76}SO_6$ (852.54): C, 76.01; H, 8.96; S, 3.76. Found: C, 75.68; H, 9.05; S, 2.56.

3. Results and discussion

3.1. Synthesis and characterization

Scheme 1 illustrates the synthetic path to PAE–PAV **5**. It starts with the synthesis of the pale yellow dialdehyde **3**, which is obtained through the Sonogashira reaction [19] of 4-formyl-2,5-dioctyloxyphenylacetylene [17c] (**1**) with 5-bromo-thiophene-2-carboxaldehyde (**2**) in 68% yield. The ^{13}C NMR spectrum (62 MHz, $CDCl_3$) of **3** is shown in Fig. 1. The subsequent Horner–Wadsworth–Emmons olefination reaction of **3** with 2,5-bis(2′-ethylhexyloxy)-*p*-xylylene-bis(diethylphosphonate) [17b] (**4**) provided polymer **5** in 37% yield after intensive work up. The dark red material shows a GPC curve peaked at $M_p = 52{,}000$ g/mol. A number-average molecular-weight, $M_n = 28{,}000$ g/mol (polydispersity index = 2.68) and a degree of polymerisation, DP = 34 were obtained. The high molecular-weight of the substance was confirmed by broad ^{1}H NMR peaks and the absence of terminal aldehyde and phosphonate signals in NMR spectra. Fig. 2 depicts the ^{13}C NMR spectrum of polymer **5**. The combination of octyloxy and 2-ethylhexyloxy as side chains makes this compound to be highly soluble in usual organic solvents. For the purpose of comparison, polymers **8** having a 2:2 triple bond/double bond ratio were also synthesized. They were obtained under the same reaction conditions starting from dialdehyde **7**. Dialdehyde **7** resulted from the Pd-catalyzed reaction of 1,4-diethynyl-2,5-dioctadecyloxybenzene (**6**) [18] with the bromo derivative **2** and was obtained in 68% yield as a yellow compound as shown in Scheme 2. Figs. 3 and 4 represent, respectively, the ^{13}C NMR spectra of dialdehyde **7** and polymer **8b**. Polymers **8** were obtained in higher yields (73–79%), however, their molecular-weights are comparatively lower (DP between 4 and 6). Longer octadecyloxy side groups were necessary for solubility reason. An attempt to synthesize polymer **12** having the same 2:2 triple bond/double bond ratio as in **8**, but with different location of the thiophene rings within the polymeric backbone, has been undertaken. As a result, the reaction of 2,5-bis(4-formyl-2,5-dioctyloxyphenylethynyl)thiophene (**10**) (obtained from the Sonogashira reaction of **1** with 2,5-dibromothiophene **9** in 60% yield after chromatographic purification) with thiophene-bis(diethylmethylene)phosphonate (**11**) led to an insoluble dark red material (Scheme 3). This was done in order to study the effect of the position of thiophene rings within the polymers backbone. Fig. 5 depicts the ^{13}C NMR spectrum of dialdehyde **9**. However, insolubility problems hindered any possible study on **12** as yet. Steps to render **12** soluble are presently undertaken and will be reported at a later stage together with its properties. Among polymers **8**, compound **8b** was selected for comparison with **5** due to its highest DP of 6 and narrowest GPC curve (PDI = 2.2).

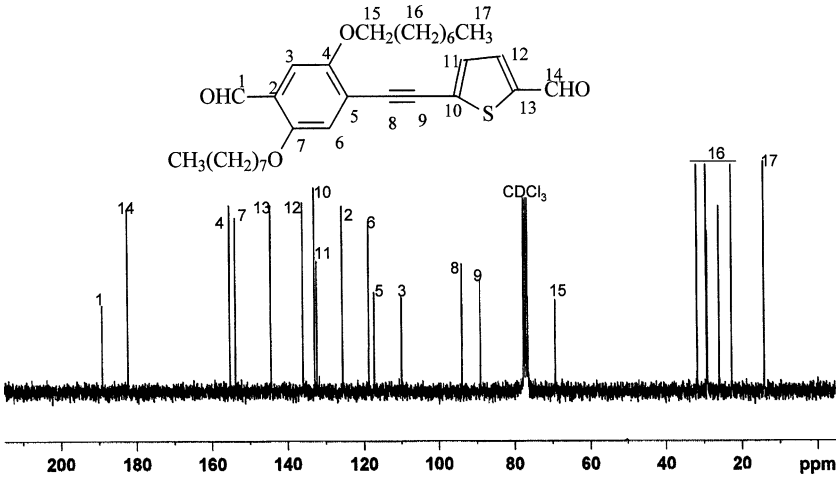

Fig. 1. ^{13}C NMR spectrum (62 MHz, $CDCl_3$) of dialdehyde **3**.

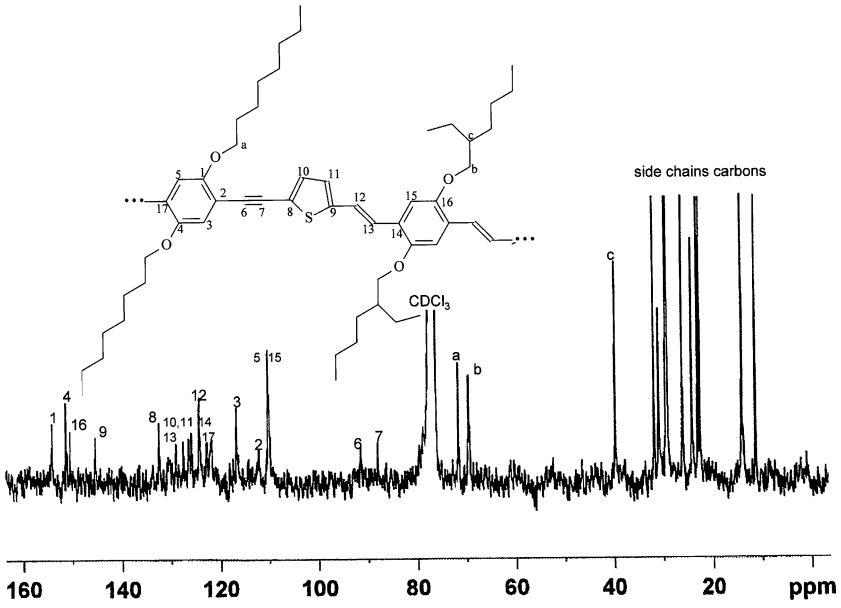

Fig. 2. ^{13}C NMR spectrum (62 MHz, $CDCl_3$) of polymer **5**.

3.2. Thermal properties

DSC thermograms recorded during the first heating run for as-polymerized samples of the four polymers revealed complex melting processes that were not perfectly reproduced during the subsequent heating cycles. Only the second heating runs, considered as reflecting the properties of the compact bulk material, are presented (Fig. 6). Polymers of the series **8** revealed pronounced reorganization ability upon cooling and the exothermic transition peaks appear rather sharp. In contrast to that, the polymers' endothermic transitions are considerably broadened and they extend on the high temperature side up to a temperature of about 100 °C above which polymers **8** are isotropic liquids, as observed by means of polarizing optical microscopy. However, no development of any characteristic optical textures were observed for polymers **8** upon cooling from isotropic state. DCS traces for **5** are nearly featureless but the optically detected birefringence was observed to decrease gradually upon heating. No liquid state was obtained for **5** that remained rubber-like material up to a temperature of about 250 °C as a result of its higher molar mass.

In order to study the structure in bulk, uniaxially oriented specimens (cylindrical filaments) have been obtained by extrusion through a conical dye [17d]. Polymers **8** could be processed at room temperature. For polymer **5**, extrusion has been performed at higher temperature (85 °C) reflecting the effect of a large increase of the molar mass on thermal properties. WAXS intensity distributions were recorded for extruded samples as functions of temperature. For the studied polymeric systems, broad peak was seen in the wide-angle regime suggesting a liquid-like short-range order in bulk. Macroscopic orientation in the transversal direction was deduced from the two-dimensional scattering patterns in which small-angle reflections at equatorial positions reflected ordering over longer distances. No clear correlation could be established between the position of these small-angle X-ray scattering intensity maxima and the length of the side chains. For instance in case of layered organizational features, the positions of the low-angle

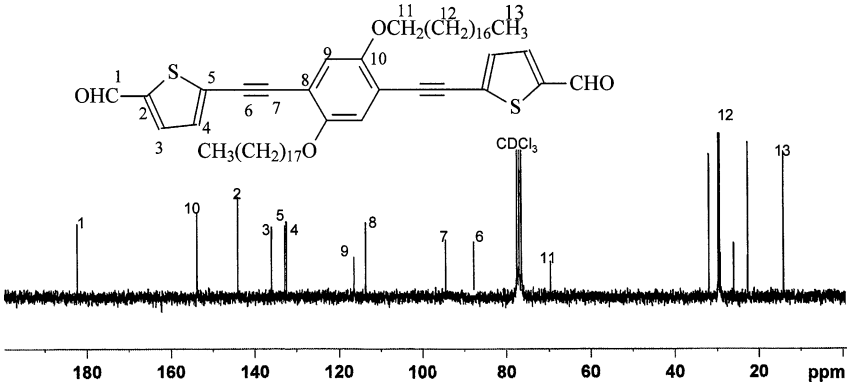

Fig. 3. ^{13}C NMR spectrum (62 MHz, $CDCl_3$) of dialdehyde **7**.

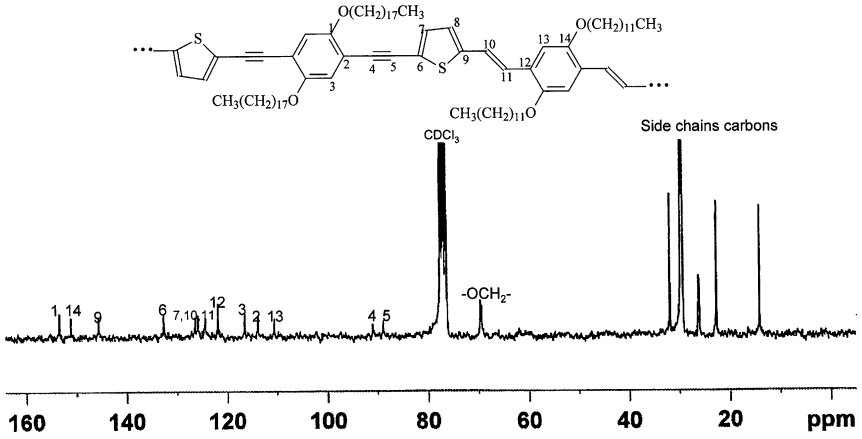

Fig. 4. ^{13}C NMR spectrum (62 MHz, $CDCl_3$) of polymer **8b**.

structure peaks are expected to shift to smaller scattering vectors with increasing side chains length and higher order reflections satisfying the ratio 1:2:3 are usually observed [17d]. The number and shape of these higher order equatorial peaks reflect the range and perfection of layered correlations. In most cases, the detection of unique low angle peak did not allow clear assignment of molecular packing. As depicted in Fig. 7, the WAXS pattern recorded at a temperature of 30 °C for **8c** shows a set of three peaks with Bragg spacings in the ratio $1:\sqrt{3}:2$, which is characteristic of hexagonal array. The figure shows that at lower temperature the low angle intensity distribution differs considerably indicating a change in the bulk morphology within this range of temperature in agreement with the thermal phase analyzed by means of DSC (Fig. 6). Long-range rectangular packing within the plane is proposed for **8c** below room temperature on the basis of comparison of positions of the intensity peaks in the small-angle range with various packing models. From a comparison of intramolecular distances with correlation distances observed in the scattering, the low-angle intensity peaks are considered as indication of backbone–backbone correlation between supramolecular aggregates made of closely packed π-conjugated backbones of PAE–PAV chains. The origin of the contrast allowing the detection of the backbone correlation may be due to different electron densities between the aromatic main chains and the aliphatic side chains. This assignment is in our opinion strongly supported by the equatorial positions of the low angle peaks, which can be attributed to the orientation of the whole macromolecular aggregates along the drawing direction when subjected to extensional flow in the course of the extrusion. Even if finer structural details could not be yet elucidated, this preliminary structural investigation shows that these macromolecular systems self-assemble to structures with a broad range of structural details depending on various parameters such as temperature, molar mass and spatial requirements of the side chains.

3.3. Photophysical studies

The photophysical behaviour of the yne-containing monomers **3**, **7** and **10** as well as the polymers **5** and **8** has been studied in dilute chloroform solutions and/or in thin solid films spin casted from chlorobenzene solutions. The optical data are given in Table 1, namely the absorption maximum, λ_a, absorption, the optical band gap energy, E_g^{opt}, the emission maximum, λ_e, the Stokes shift, the full-width-at half-maximum of the emission, $fwhm_e$ and the fluorescence quantum yield, Φ_f. Fig. 8 depicts the absorption and emission spectra of the monomeric dialdehydes **3**, **7**, **10**. As expected the single ethynylated compound **3** exhibits a higher energy π–π* transition ($\lambda_a = 401$ nm) than its double ethynylated congeners **7** ($\lambda_a = 415$ nm) and **10**

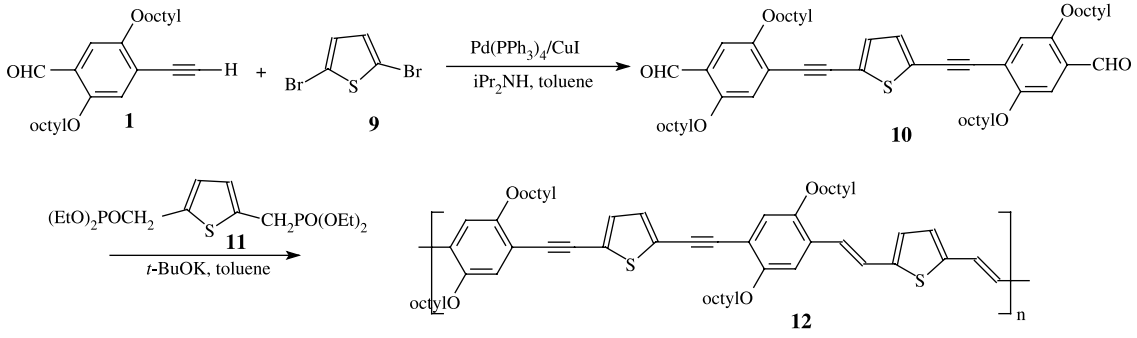

Scheme 3.

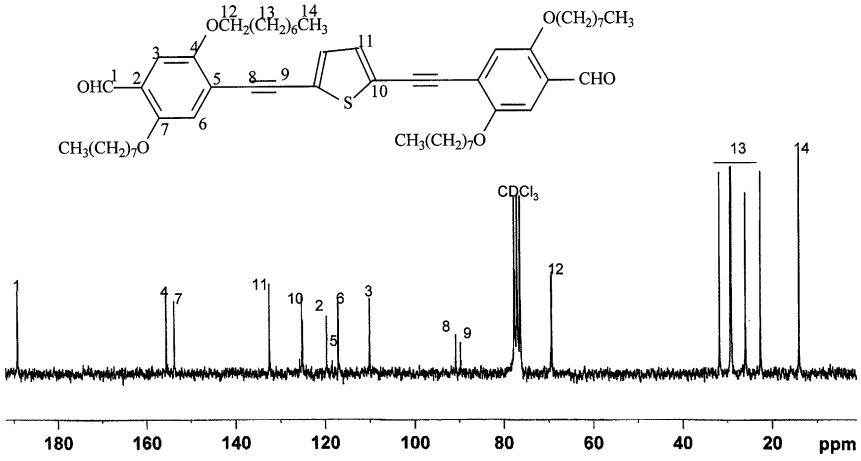

Fig. 5. ^{13}C NMR spectrum (62 MHz, $CDCl_3$) of dialdehyde **10**.

Table 1
Optical data of monomers **3**, **6** and **10** and polymers **5** and **8b** in dilute $CHCl_3$ solution and in thin solid film

Code	λ_a (nm)[a]	E_g^{opt} (eV)	λ_e (nm)[a]	Stokes shift (nm (cm^{-1}))	$fwhm_e$ (nm (cm^{-1}))	Φ_f (%)[b]
3[c]	350, 401	2.74	462	61 (3300)	68 (3000)	24
7[c]	346, 415	2.62	483	68 (3400)	74 (3000)	31
10[c]	419	2.68	459, 486	40 (2100)	48 (2200)	41
5[c]	486	2.27	542, 583	56 (2100)	55 (1800)	46
8b[c]	475	2.31	535, 576	60 (2400)	67 (2200)	51
5[d]	501, 531	2.06	568, 608	67 (2300)	75 (2200)	7
8b[d]	501, 535	2.13	–	–	–	~0

[a] Underlined value corresponds to the maximum of the hyperchromic band.
[b] Φ_f-value $\pm$10%.
[c] In dilute chloroform solution (conc. 10^{-5}–10^{-6} M).
[d] Thin solid films of thicknesses between 100 and 150 nm spin casted from chlorobenzene solution and dried at 80 °C for 8 h.

(λ_a=419 nm). The absorption trace of **3** consists additionally of a hyperchromic peak at 350 nm attributed to the presence of alkoxy side chains [20]. The intensity of this peak reduces with the extension of conjugation in **7**

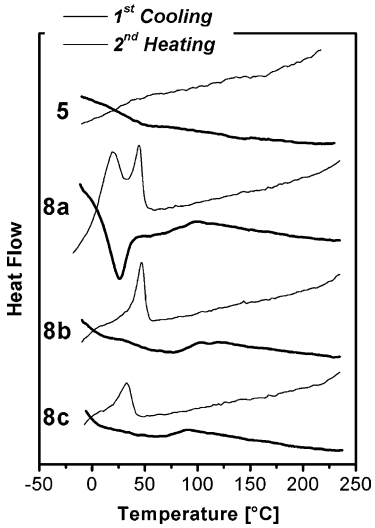

Fig. 6. DSC thermograms as recorded for the bulk polymers during first cooling and second heating runs with the rate 10 °C/min.

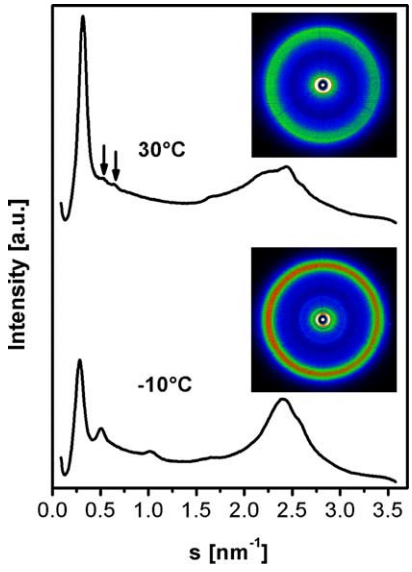

Fig. 7. WAXS intensity distributions vs. the scattering vector as recorded for polymer **8c** at temperatures of (top) 30 and (bottom) −10 °C. The insets show the corresponding 2D WAXS patterns. The arrows in the intensity distribution recorded at 30 °C indicate positions of the intensity maxima satisfying the ratio $\sqrt{3}$: 2 from the first intensity maximum.

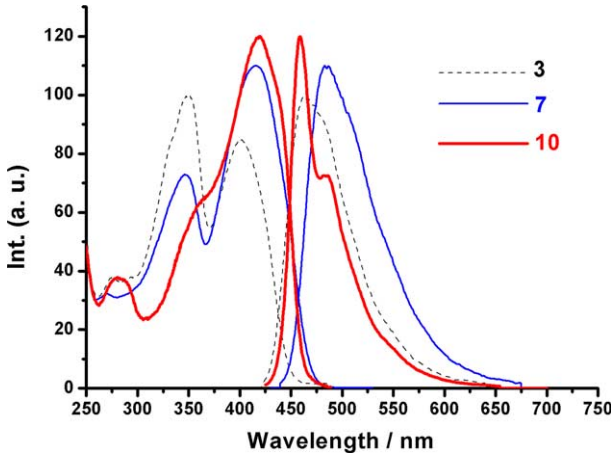

Fig. 8. Normalized absorption and normalized emission spectra of dialdehydes **3**, **7** and **10** in dilute chloroform solution.

(346 nm) as well as in **10**, where it appears as a shoulder around 355 nm. The higher degree of bending and other motions combined with enhanced backbone planarization at first singlet excited state, S_1, of **3** and **7**, ascribed to the presence of less side chains compared to **10**, is at the source of their less structured, broader ($fwhm_e = 3000\ cm^{-1}$) and red shifted emission bands centered at $\lambda_e = 462$ nm for **3** and at $\lambda_e = 483$ nm for **7**. The fourfold alkoxy-substituted compound **10** is characterised with the smallest Stokes shift of 2100 cm^{-1} and a well structured emission spectrum showing a 0–0 transition at 459 nm and a 0–1 transition at 486 nm ($fwhm_e = 2200\ cm^{-1}$). The fluorescence quantum yields of thiophene-containing dialdehydes (0.2–0.4) are low compared to their solely phenyl-containing counterparts, whose Φ_f-values are close to unity. This might be attributed to heavy atom effects [17a].

The dilute solution absorption and emission spectra of the polymers **5** and **8** are shown in Fig. 9. The absorption and emission spectra of polymer **5** ($\lambda_a = 486$ nm, $\lambda_e = 542$ nm) are red shifted compared to those of polymers **8** ($\lambda_a = 475$ nm, $\lambda_e = 535$ nm). Their well structured emission spectra consist additionally of a 0–1 transition band at $\lambda_e = 583$ nm for **5** and

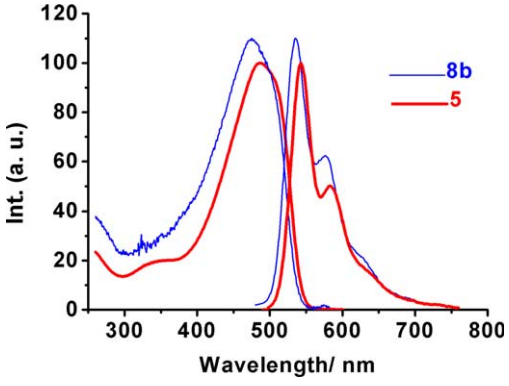

Fig. 9. Normalized absorption and normalized emission spectra of polymers **5** and **8b** in dilute chloroform solution.

$\lambda_e = 576$ nm for **8**. Solution fluorescence quantum yields around 50% were obtained for both types of materials.

Contrary to the solutions, both **5** and **8** show identical absorptive behaviour in thin film (Fig. 10 left). Their solid state absorption spectra consist of two maxima centered around 501 and 531 nm. Optical band gap energies of ca. 2.10 eV were obtained. In contrast a great disparity is observed in their solid state emissive behaviour (Fig. 10 right). While polymer **5** has a thin film fluorescence spectrum, which is similar in shape to that in solution, but red shifted, and consisting of a 0–0 transition at $\lambda_e = 568$ nm and a 0–1 transition at $\lambda_e = 608$ nm, all three polymers **8** exhibit a very broad and structureless fluorescence bands of extremely low intensity. The lack of fluorescence in thin films of **8** ($\Phi_f \sim 0\%$) suggests very strong π–π interchain interactions, source of diverse radiationless pathways, resulting from the presence of two –C≡C– units within the constitutional unit of **8**, which strongly contribute in enhancing the backbone planarization in the excited state. Another major source of fluorescence quenching is the presence of sulphur atoms (heavy atom effects) [17a], which would explain the low Φ_f -value of 7% obtained for **5**.

3.4. Electrochemical studies

The electrochemical behaviour of the polymers was investigated by the combination of cyclic voltammetry (CV) and electrochemical voltage spectroscopy (EVS). CV and EVS were performed in a solution of Bu_4NClO_4 (98%, ~0.1 M) in anhydrous acetonitrile at a scan rate of 10 mV/s. A platinum electrode coated with a thin polymer film was used as the working electrode. A Pt foil served as the counter electrode and an Ag/AgCl electrode was used as the reference electrode.

Fig. 11 gives the CV curves of **5** and **8b**. The vertical lines show the redox onset values as obtained through EVS. The electrochemical data of the polymers are given in Table 2. All the potential values shown are versus normal hydrogen electrode (NHE). NHE-level in the Fermi scale used for HOMO-LUMO calculation was −4.75 eV [21,22].

Both p- and n-doping processes were reversible in both **5** and **8b**. Identical oxidation onset potential, E^{ox}_{onset}, of 680 mV was obtained leading to a HOMO-level of −5.43 eV for both polymers. However, polymer **8b** exhibits an oxidation peak potential, E^{ox}_{peak}, of 1075 mV, which is 185 mV higher than that of **5** due to its higher number of triple bond units per repeating unit. Onset reduction potentials, E^{red}_{onset}, of −1610 mV for **5** and −1590 mV for **8b** were obtained, leading, respectively, to LUMO-levels of −3.14 and −3.16 eV. The differences of 0.02 eV of the LUMO-levels and of 10 mV of the reduction peak potentials, E^{ox}_{peak}, i.e. −1780 mV for **5** and −1790 mV for **8b**, are within the range of error. It is evident from the above results that almost identical electrochemical behaviour is obtained in both polymers. The inset in Fig. 11 presents the HOMO–LUMO energy diagram of the

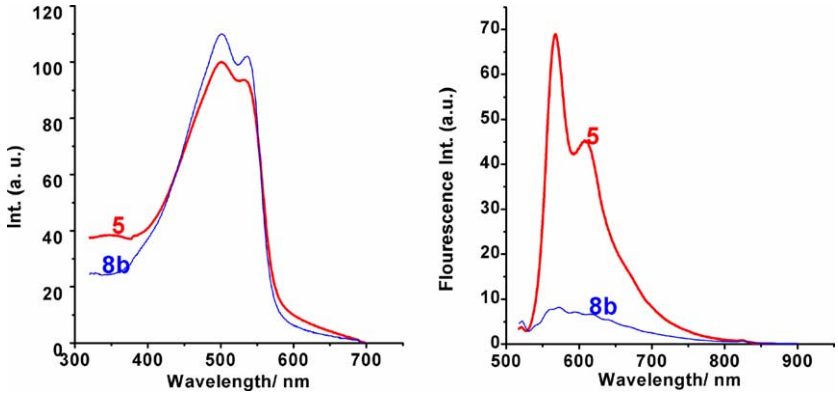

Fig. 10. Normalized absorption spectra (left) and emission spectra (right) of polymers **5** and **8b** in thin film.

Table 2
Electrochemical data from polymers **5** and **8b** as obtained from cyclic voltammetry (CV) and electrochemical voltage spectroscopy (EVS)

Code	E^{ox}_{onset} (mV)	E^{red}_{onset} (mV)	E^{ox}_{peak} (mV)	E^{ox}_{peak} (mV)	HOMO (eV)	LUMO (eV)	E^{ec}_{g} (eV)
5	+680	−1610	+890	−1780	−5.43	−3.14	2.29
8b	+680	−1590	+1075	−1790	−5.43	−3.16	2.27

All potentials are given vs. normal hydrogen electrode (NHE). NHE-level used for HOMO–LUMO calculation was −4.75 eV [12].

polymers. An electrochemical band gap energy, E^{ec}_{g}, of ~2.28 eV was obtained, leading to a discrepancy to the optical energy gap of ~0.18 eV. Such discrepancy is caused by the insulating effect of the side chains during the electrochemical process [12,23–25].

3.5. Photovoltaic studies

Photovoltaic devices of configuration ITO/PEDOT:PSS/active layer/LiF/Al were studied under AM1.5 conditions. The active layer consisted of either polymer **5** or **8b** as donor component and the C_{60}-derivative 1-(3-methoxycarbonyl) propyl-1-phenyl [6,6] C_{61} (PCBM) as acceptor, mixed together in a 1:3 ratio. Fig. 12 depicts the *I–V* curves of cells from polymers **5** and **8b**. The photovoltaic parameters of three cells from each of the two polymers are summarised in Table 3. It is obvious from the obtained data that devices designed from polymer **5** show far better characteristics than those from polymer **8b**. They exhibit open circuit voltages, V_{OC}, as high as 900 mV and filling factors, FF, around 50%; but low short circuit currents, I_{SC}, around 2.5 mA/cm^2 were obtained leading to power conversion efficiencies between 1 and 1.2%. Actions to optimize the device parameters, especially to increase the I_{SC}, are currently on the way and the results will be reported elsewhere in the nearest future. The best and largest cell from **8b** has following characteristics: V_{OC} = 500 mV, I_{SC} = 1.44 mA/cm^2, FF = 37.1% and $\eta_{AM1.5}$ = 0.27%. The main limiting factors in this case are, apart from the comparatively (to **5**) lower molecular weight [26], (1) the higher number of –C≡C–units [11,15] within the backbone of **8b** together with (2) the longer octadecyl and dodecyl side

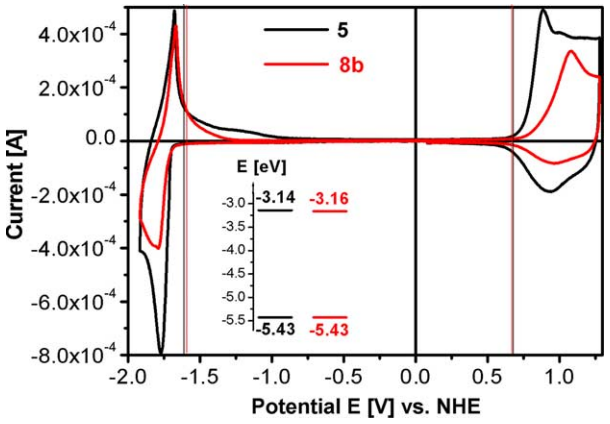

Fig. 11. CV-curves of polymers **5** and **8b**. The vertical lines show the redox onset values as obtained by EVS. The inset is the position of the HOMO and LUMO levels in the Fermi energy scale.

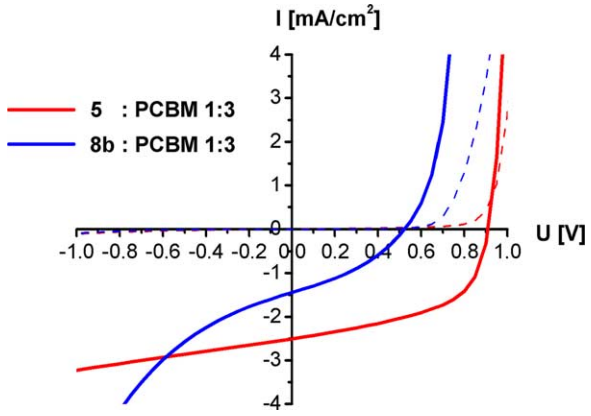

Fig. 12. Current–voltage (*I–V*) curves of **5** and **8b** solar cells in dark (dash) and under illumination (solid line) with white light at irradiation intensity of 100 mW/cm^2.

Table 3
Photovoltaic parameters from devices of configuration: ITO/PEDOT/polymer: PCBM (1:3)/LiF/Al

Code	Active area (mm^2)	V_{OC} (mV)	I_{SC} (mA/cm^2)	FF (%)	$\eta_{AM1.5}$ (%)
5	10.2	900	2.51	53.7	1.21
5	15.3	900	2.44	50.6	1.11
5	11.6	800	3.21	46.3	1.19
8b	10.8	500	1.46	35.8	0.26
8b	16.2	500	1.44	37.1	0.27
8b	10.2	600	1.15	36.8	0.25

chains [25]. The analysis of the data showed that morphology of the polymer film and length of the main chain influence the operation voltage of the devices. The higher number of triple bonds, on the one hand, not only slow the mobility of the photogenerated charges [12] but also enables strong π–π interchain interactions among the polymeric chains of **8b** as already demonstrated above, thereby limiting the interfacial area between donor and acceptor particles. The longer side chains in **8b** on the other hand, not only also contribute to limiting the interfacial area but also favour an easy recombination of the photogenerated charges by elongating their percolating path to the electrodes [25].

4. Conclusions

The synthesis of two classes of thiophene-containing PAE–PAV having either a 1:2 (in **5**) or a 2:2 (in **8**) triple bond/double bond ratio within the repeating units has been carried out. Both types of compounds show identical absorption behaviour in the solid state; optical band gap energies around 2.10 eV were obtained. In contrast great disparity in their emissive behaviour was observed. While a clear and well-structured fluorescence spectrum was obtained for **5** with a fluorescence quantum yield around 7%, a total fluorescence quenching was observed in all three polymers **8**, as a result of both higher number of triple bonds and higher number of thiophene rings (heavy atom effects) in **8**. The shorter side chains and less –C≡C– units in **5** together with its higher molecular weight [26] led to better PV parameters from cells designed from **5** than from **8b**. V_{OC} as high as 900 mV, FF around 50%, I_{SC} around 2.5 mA/cm^2 and efficiencies between 1 and 1.2% were obtained. An improvement of the short circuit current and consequently enhancement of the efficiency through morphological treatment of the devices is currently under study and will be reported in a later stage. Moreover, establishing (or predicting) a correlation between the HOMO/LUMO energy levels and the photovoltaic parameters (such as V_{OC}), as has been done with other polymer systems of PPV-type [27,28], is not possible in this present situation [25].

References

[1] Brabec CJ, Sariciftci NS, Hummelen JC. Adv Funct Mater 2001; 11:15.
[2] Hoppe H, Sariciftci NS. J Mater Res 2004;19:1924.
[3] (a) Winder C, Sariciftci NS. J Mater Chem 2004;14:1077.
(b) Drees M, Heflin JR, Davis RM, Topasna D, Stevenson P. Proc SPIE 2004;5215:89.
[4] Kietzke T, Neher D, Landfester K. Nat Mater 2003;2:408.
[5] Sariciftci NS, Smilowitz L, Heeger AJ, Wudl F. Science 1992;258: 1789.
[6] Brabec CJ, Zerza G, Cerullo G, De Silvestri S, Luzzati S, Hummelen JC, et al. Chem Phys Lett 2001;340:232.
[7] Padinger F, Rittberger RS, Sariciftci NS. Adv Funct Mater 2003;13:1.
[8] Sirringhaus H, Brown PJ, Friend RH, Nielsen MM, Bechgaard K, Langeveld-Voss BMW, et al. Nature 1999;401:685.
[9] Dimitrakopoulos CD, Mascaro DJ. IBM J Res Dev 2001;45:11.
[10] Shaheen S, Brown K, Miedaner A, Curtis C, Parilla P, Gregg B, et al. NCPV and solar program review meeting, NREL/CD-520-333586 2003: p. 438–41.
[11] Sensfuss S, Konkin A, Al-Ibrahim M, Nazmutdinova G, Roth HK, Zhokhavets U, et al. Proc SPIE 2004;5215:129.
[12] Egbe DAM, Kietzke T, Carbonnier B, Mühlbacher D, Hörhold HH, Neher D, et al. Macromolecules 2004;37:8863.
[13] Hoppe H, Egbe DAM, Mühlbacher D, Sariciftci NS. J Mater Chem 2004;14:3462.
[14] Konkin AL, Sensfuss S, Roth HK, Nazmutdinova G, Schroedner M, Al-Ibrahim M, et al. Synth Met 2005;148:199.
[15] Al-Ibrahim M, Konkin A, Roth HK, Egbe DAM, Klemm E, Zhokhavets U, et al. Thin Solid Films 2005;474:201.
[16] Egbe, DAM, Sell S, Ulbricht C, Voigt S. www.e-polymers.org/paris/data/L1286.pdf.
[17] (a) Egbe DAM, Tillmann H, Birckner E, Klemm E. Macromol Chem Phys 2001;202:2712.
(b) Egbe DAM, Roll CP, Birckner E, Grummt UW, Stockmann R, Klemm E. Macromolecules 2002;35:3825.
(c) Egbe DAM, Bader C, Nowotny J, Günther W, Klemm E. Macromolecules 2003;36:5459.
(d) Carbonnier B, Pakula T, Egbe DAM. J Mater Chem 2005;15:880.
[18] Egbe DAM, Klemm E. Macromol Chem Phys 1998;199:2683.
[19] (a) Sonogashira K, Tohda Y, Hagihara N. Tetrahedron Lett 1975;50: 4467.
(b) Bunz UHF. Chem Rev 2000;100:1605.
[20] Grummt UW, Birckner E, Klemm E, Egbe DAM, Heise B. J Phys Org Chem 2000;13:112.
[21] Gomer RJ, Tryson G. J Chem Phys 1977;66:4413.
[22] Kötz R, Neff H, Müller K. J Electroanal Chem 1986;215:331.
[23] Chen ZK, Huang W, Wang LH, Kang ET, Chen BJ, Lee CS, et al. Macromolecules 2000;33:9015.
[24] Yamamoto T, Lee B-L. Macromolecules 2002;35:2993.
[25] Egbe DAM, Nguyen LH, Hoppe H, Mühlbacher D, Sariciftci NS. Macromol Rapid Commun 2005;26:1389.
[26] Schilinsky P, Asawapirom U, Scherf U, Biele M, Brabec CJ. Chem Mater 2005;17:2175.
[27] Kim H, Jin SH, Suh H, Lee K. Proc SPIE 2004;5215:111.
[28] Hoppe H, Sariciftci NS, Egbe DAM, Mühlbacher D, Koppe M. Mol Cryst Liq Cryst 2005;426:255.